Chapter 6
Financing Climate Change Policies: A Multi-phase Integrated Assessment Model for Mitigation and Adaptation

Willi Semmler, Helmut Maurer, and Tony Bonen

JEL Classification: C61 · Q54 · Q58 · H5

6.1 Introduction

This paper extends the novel numerical modelling of optimal climate change policy responses developed in Semmler et al. [15]. In that paper, the dynamic decision problem was solved under a single regime of fixed exogenous parameters. We extend that framework here to consider multiple regimes. Under updated parameterizations, we compare the single-regime model against a multi-regime specification in which a new climate financing mechanism—"green bonds"—are introduced to the policy set. The regimes are exhaustive and sequential meaning, there is no possibility of the model returning to an earlier phase. In order to solve the multi-regime model a new numerical algorithm is applied: the arc parameterization method (APM). APM ensures continuous trajectories of the model's state variables, making the numerical

This paper was developed while Willi Semmler was a visiting scholar at the IIASA in July and August 2016. He would like to thank the IIASA for its hospitality. A related version of this paper was worked out while Willi Semmler was a visiting scholar at the IMF Research Department in April 2016. The authors would like to thank Prakash Loungani and his colleagues for many helpful insights.

W. Semmler
New School for Social Research, Henry Arnold Professor of Economics, New York, NY, USA

H. Maurer
Institute for Analysis and Numerics, University of Münster, Müntser, Germany

T. Bonen (✉)
Labour Market Information Council, Ottawa, Canada
e-mail: tony.bonen@lmic-cimt.ca

J. L. Haunschmied et al. (eds.), *Dynamic Economic Problems with Regime Switches*, Dynamic Modeling and Econometrics in Economics and Finance 25,
https://doi.org/10.1007/978-3-030-54576-5_6

solution more realistic. We find that the multi-regime model is Pareto-superior to the single-regime version.

The multi-regime model builds on the structure in Semmler et al. [15], which develops an integrated assessment model (IAM) of climate change's impact on social welfare. In that paper, the finite-horizon model continually solves for the optimal financing allocation to three climate change policy responses: (i) mitigation of increased CO_2 emissions; (ii) adaptation to the unavoidable consequences of climate change and (iii) investment in carbon-neutral, productivity-enhancing infrastructure. Under various sensitivity tests, the consistent optimal solution was found to prioritize funding of the latter category—productivity-enhancing infrastructure—to a much greater extent than the other two policy areas (i.e. over 90% of the total budget).

This policy-focused IAM is extended here to include a new public finance mechanism—so-called "green bonds"—designed to support climate change policy action. The funds raised by green bonds must be allocated to environmental efforts (i.e. among the three allocation options) and are repaid over very long horizons. As argued by Sachs [14], Flaherty et al. [6] and Heine et al. [7], such green bond financing generates more equitable intergenerational outcomes. Intergenerational equity is improved because repayment of the green bonds is a cost faced by future generations who will reap the benefits of an economy spared the worst of climate change's impacts as a result of policies undertaken by earlier generations. It follows that at least two model regimes are required: a period of green bond issuance and a period of their repayment. We also include an antecedent regime in which green bonds do not exist; this represents the current policy world and is similar to the single-regime model in Semmler et al. [15]. We show that the introduction of green bonds reduces total emissions, increases private and public capital, and results in higher overall welfare.

The remainder of the paper is organized as follows. Section 6.2 describes the general form of the IAM. Section 6.3 describes the numerical solution techniques. Sections 6.4 and 6.5 present the results for the single-regime model and its multi-regime extension, respectively. Section 6.6 reports on sensitivity analyses applied to the multi-regime model. Section 6.7 concludes.

6.2 Model Description

Climate change economic models are complex dynamic systems that typically do not lend themselves to standard, closed-form solutions. Common work arounds include linearizing the dynamic system or generating exogenous macroeconomic trajectories that are later integrated with climate dynamics.[1] In contrast, our integrated assessment model (IAM) numerically determines optimal control solutions for the full dynamic system. The model described below extends the IAM developed in

[1] See Bonen et al. [2] for a further discussion.

Semmler et al. [15]. Note that in spite of the use of capital letters, all variables are in per capita terms.

The dynamic system is driven by the state variables $X = (K, R, M, b, g) \in \mathbf{R^5}$ as defined by the following equations:

$$\dot{K} = Y \cdot (\nu_1 g)^{\beta}(1 - \tau_k) - C - e_P - (\delta_K + n)K - u\,\psi R^{-\zeta}, \tag{6.1}$$

$$\dot{R} = -u, \tag{6.2}$$

$$\dot{M} = \gamma u - \mu(M - \kappa\widetilde{M}) - \theta(\nu_3 \cdot g)^{\phi}, \tag{6.3}$$

$$\dot{b} = (r_t - n)b - \alpha_4 e_P - Y \cdot (\nu_1 g)^{\beta}\tau_k + \varsigma_k g, \tag{6.4}$$

$$\dot{g} = \alpha_1 e_P - (\delta_g + n)g + \varsigma_k g, \tag{6.5}$$

where K is the stock of private capital, R is the stock of the non-renewable resource, M is the atmospheric concentration of CO_2, b is the public debt level and g is the stock of public capital. Note that it is from g that climate policy actions are funded.[2]

The dynamic system in (6.1)–(6.5) extends Semmler et al. [15] by introducing $k > 1$ regimes. Specifically, τ_k and ς_k are regime-specific parameters that define three regimes ($k = 1, 2, 3$). When $\tau_k = \varsigma_k = 0$ there are no green bonds in circulation. For $\varsigma_k > 0$, green bonds are issued and the funds allocated to the stock of public capital used for climate change action, g. When $\tau_k > 0$, a special income tax is levied to pay down public debt, b.

The accumulation rate of private capital $\dot{K}$ is driven by, among other factors, output generated under a CES production function in which K and the extracted non-renewable resource u are inputs,

$$Y(K, u) := A(A_K K + A_u u)^{\alpha}. \tag{6.6}$$

Here A is multifactor productivity, A_K and A_u are efficiency indices of the inputs K and u, respectively. In (6.1) private-sector output Y is modified by the infrastructure share allocated to productivity enhancement $\nu_1 g$, for $\nu_1 \in [0, 1]$. This public-private interaction generates gross output $Y(\nu_1 g)^{\beta}$.[3] When green bonds are being repaid, $\tau_k > 0$ reduces net output to $Y(\nu_1 g)^{\beta}(1 - \tau_k)$, from which the economy consumes C, pays a lump sum tax e_P, and is subject to physical δ_K and demographic n depreciation. The last term in (6.1) is the opportunity cost of extracting the non-renewable resource u, where ψ and ζ are the scale and shape parameters that tie the marginal cost of u to the remaining stock of the resource à la Hotelling [9].

The dynamics $\dot{R}$ and $\dot{M}$ specify the environmental drivers of climate change. Equation (6.2) is the stock of the non-renewable resource R depleted by u units in each period. The depletion rate is constrained such that $0 \leq u(t) \leq 0.1, \forall t$. Equation (6.3) defines the change of CO_2, which is affected nonlinearly by mitigation efforts,

[2] All variables are in per capita terms.

[3] The exponent β is the output elasticity of public infrastructure, $\nu_1 g$.

$\nu_3 g$.[4] The non-renewable resource emits carbon dioxide and thus increases the atmospheric concentration of CO_2 at the rate γ. The environmentally stable level of CO_2 concentration is $\kappa > 1$ times the pre-industrial level $\widetilde{M}$. CO_2 levels at or below this level are naturally re-absorbed into the ecosystem (e.g. oceanic reservoirs) at the rate μ. The last term in (6.3) is the reduction of per-period emissions $\dot{M}$ due to the allocation of $\nu_3 \in [0, 1]$ of public infrastructure g to mitigation projects.

The dynamics $\dot{b}$ and $\dot{g}$ specify the government's fiscal stance. Revenue is generated from the lump sum tax e_P and the regime-specific income tax used to repay green bonds, τ_k. The latter flows directly to debt repayment. The former is allocated among shares $\sum_{i=1}^{4} \alpha_i = 1$: capital accumulation α_1, social transfers α_2 and administrative overhead $\alpha_3 > 0$. The remainder $\alpha_4 = 1 - \alpha_1 - \alpha_2 - \alpha_3$, pays down the stock of debt. Further, we constrain the lump sum tax to be $0 \leq e_P \leq 1, \forall t$.

In addition to repayments $\alpha_4 e_P$ and τ_k, public sector surplus/deficit $\dot{b}$ in (6.4) is driven by the time-varying interest rate r_t, and green bond issuances $\varsigma_k g$. The growth of public capital, Eq. (6.5), evolves according to the revenue stream $\alpha_1 e_P$ and funds raised from green bond issuance $\varsigma_k g$, but depreciates at the population-adjusted rate of $\delta_g + n$.

The objective function is the economy's per capita social welfare. Welfare W is maximized over a given planning horizon $[0, T]$, where $T > 0$ denotes the terminal time. Using a CES welfare function, welfare is a function of T, state variables $X \in \mathbf{R^5}$ and control variables U:

$$W(T, X, U) = \int_0^T e^{-(\rho - n)t} \frac{\left(C \cdot (\alpha_2 e_P)^\eta \left(M - \widetilde{M}\right)^{-\epsilon} (\nu_2 g)^\omega\right)^{1-\sigma} - 1}{1 - \sigma} \, dt. \quad (6.7)$$

Private consumption C is augmented by three factors: (i) the share $\alpha_2 \in [0, 1]$ of tax revenue e_P used for direct welfare enhancement (e.g. healthcare, social services); (ii) the amount by which atmospheric concentration of CO_2 M is above the pre-industrial level $\widetilde{M}$ and (iii) the share $\nu_2 \in [0, 1]$ of public infrastructure g allocated to climate change adaptation. Exponents $\eta, \epsilon, \omega > 0$ ensure social expenditures and adaptation are welfare enhancing, whereas carbon emissions produce a disutility.[5] Finally, the pure discount rate ρ is adjusted by the population growth rate n.

The policymaker maximizes (6.7) subject to (6.1)–(6.5) via the control vector

$$U = (C, e_P, u, \nu_1, \nu_2, \nu_3) \in \mathbf{R^6}. \quad (6.8)$$

[4]Use of R emits carbon dioxide increasing M at the rate γ. The stable level of CO_2 emissions is $\kappa > 1$ of the pre-industrial level $\widetilde{M}$. Some CO_2 is absorbed into oceanic reservoirs at the rate μ.

[5]Note that instead of an independent damage function mapping climate change into output reductions, (6.7) treats climate change as a direct welfare loss. Adaptation efforts are modelled in a similarly direct fashion. We adopt this approach because the welfare impacts of climate change are not limited to lost productivity. For example, loss of life will increase from changing disease vectors and more intense heat waves.

Table 6.1 Definition of climate change policy funding shares

Variable	Definition	In equations
ν_1	Investment in carbon-neutral private infrastructure	$\dot{K}$ (6.1) and $\dot{b}$ (6.4)
ν_2	Climate change adaptation. Funds used to increase the population's resilience to climate change	W (6.7)
ν_3	Climate change mitigation. Funds used to reduce CO_2 emissions	$\dot{M}$ (6.3)

As noted, C is per capita consumption, e_P is a tax on capital gains and the rate of non-renewable resources extracted per period is u. The control variables ν_1, ν_2 and ν_3 determine the allocation of public capital g to carbon-neutral private capital, climate change adaption and climate change mitigation efforts, respectively (see Table 6.1).[6] As shares of $g, \nu_i \in [0, 1],\ i = 1, 2, 3$ are constrained by $\sum_{i=1}^{3} \nu_i = 1$, total climate change policy funding levels are therefore $\nu_1 g$, $\nu_2 g$ and $\nu_3 g$.

All parameters for the model defined in Eqs. (6.1) through (6.7) are listed in Table 6.2.

6.3 Numerical Solution Techniques

The control problem is discretized on a fine grid, generating a large-scale nonlinear programming problem which is formulated with the Mathematical Programming Language AMPL; see Fourer et al. (1993). In AMPL we employ the interior-point optimization solver IPOPT (see Wächter and Biegler, 2006), that furnishes the control and state variables as well as the adjoint (co-state) variables. In this way, we are able to check whether we have found an *extremal solution* satisfying the necessary optimality conditions. To this end, we first derive an analytical expression of the control as a function of state and adjoint variables via the Maximum Principle. Inserting the computed values of state and adjoint variables into this analytical expression, the values must agree with the directly computed control values with a given tolerance. To verify sufficient conditions for local optimality, we could apply the second-order sufficient conditions presented in Augustin and Maurer [1]. This test amounts to verifying that an associated matrix Riccati equation has a bounded solution. However, since this is a rather elaborate procedure, we refrain from performing this test.

The IPOPT solver is sufficient for single-regime models and was implemented for the solutions reported in Semmler et al. [15]. For the multi-regime extension we introduce a novel application of the arc parameterization method (APM). In Sect. 6.5.3 we show that the APM approach produces realistic trajectories that are Pareto-superior to those of the single-regime model. Below we provide a brief description of the arc parameterization method. A full explanation of APM is offered in Appendix.

[6] Under a single-regime setting, Semmler et al. [15] demonstrate incorporating the ν_i as controls in U improves welfare outcomes versus treating them as fixed parameters.

Table 6.2 Parameter values

Variable	Value	Definition
ρ	0.03	Pure discount rate
n	0.015	Population growth rate
η	0.1	Elasticity of transfers and public spending in utility
ϵ	1.1	Elasticity of CO_2-eq concentration in (dis)utility
ω	0.05	Elasticity of public capital used for adaptation in utility
σ	1.1	Intertemporal elasticity of instantaneous utility
A	1	Total factor productivity
A_K	1	Efficiency index of private capital
A_u	100	Efficiency index of the non-renewable resource
α	0.05	Output elasticity of privately owned inputs, $(A_k K + A_u u)^{\alpha}$
β	0.5	Output elasticity of public infrastructure, $\nu_1 g$
ψ	0.1	Scaling factor in marginal cost of resource extraction
ζ	2	Exponential factor in marginal cost of resource extraction
δ_K	0.075	Depreciation rate of private capital
δ_g	0.05	Depreciation rate of public capital
α_1	0.1	Proportion of tax revenue allocated to new public capital
α_2	0.7	Proportion of tax revenue allocated to transfers and public consumption
α_3	0.1	Proportion of tax revenue allocated to administrative costs
r_t	0.07	Interest rate charged on debt, fixed $\forall t$
$\widetilde{M}$	1	Pre-industrial atmospheric concentration of greenhouse gases
γ	0.9	Fraction of greenhouse gas emissions not absorbed by the ocean
μ	0.01	Decay rate of greenhouse gases in atmosphere
κ	2	Atmospheric concentration stabilization ratio (relative to $\widetilde{M}$)
θ	0.01	Effectiveness of mitigation measures
ϕ	1	Exponent in mitigation term $(\nu_3\, g)^{\phi}$

6.3.1 Application of Arc Parameterization

Multi-process (multi-phase) optimal control problems have been studied by Clarke and Vinter [4, 5] and later by Augustin and Maurer [1]. To solve our optimal multi-phase control problem, we implement the arc parameterization presented in Maurer et al. [12], Loxton et al. [11] and Lin et al. [10], along with discretization and nonlinear programming methods used previously. Although Maurer et al. [12] apply the arc-parametrization method (APM) only to bang-bang control problems, the APM is extended here to a continuous, multi-phase control problems (see Appendix for further details).

Following this work, we define the multi-process control problem on a grid of $t \in [0, T]$ with $s+1$ phases (regimes) occurring at switch points $t_k \in (0, T),\ k = 1, ..., s$. Discretization is achieved via a uniform grid of mesh points

$$\tau_i = i \cdot h, \quad h = \frac{1}{N}, \quad i = 0, 1, \ldots, N.$$

The mesh size N must be a multiple of the number $s+1$ of intervals. This condition ensures that the phase boundaries $(k+1)/(s+1),\ k = 0, \ldots, s+1$, appear as knot points in the applied integration schemes. The resulting discretized control problem is then formulated as a large-scale nonlinear programming problem (NLP) in AMPL.

We define multiple regimes on the specified mesh grid as $s+1$ ordinary differential equations. Let the dynamics of the economic process in the interval $[t_k, t_{t+1}]$ be given by

$$\dot{x}(t) = f_k\big(x(t), u(t)\big), \quad t_k \leq t \leq t_{k+1} \quad (k = 0, 1, \ldots, s), \tag{6.9}$$

where the right-hand side of the ODE is a C^1 function.

A *continuous* state trajectory $x(t)$ on the entire interval $[0, T]$ is obtained by imposing the continuity condition

$$x(t_k) = x(t_k-), \qquad k = 1, \ldots, s. \tag{6.10}$$

Note that the continuity of the state variables in (6.10) does not automatically ensure the continuity of the control variables; in fact, these can jump when the system transitions between policy phases.

6.4 Single-Phase Model

The model defined in Eqs. (6.1)–(6.7) is discretized on a fine grid $t \in [0, 70]$. While each integer step can be said to represent one year, discrete steps are set at $\Delta t = 0.05$ for the single-phase model, ie., we use $N = 1400$ grid points. For the multi-phase model, subsequently discussed, we also use $N = 1400$ or a refined grid. The finer grid helps the multi-phase pathways be smoother than otherwise. Importantly, the single-phase model does not allow for green bonds or a new tax for repayment. Therefore, the parameters are set at $\varsigma_k = \tau_k = 0$ in Eqs. (6.1), (6.4) and (6.5) for the single-phase model.

The numerical solution technique employed in AMPL requires initial values for each state variable. In addition, model stability is ensured by placing terminal value boundaries (maxima or minima) on certain state variables. The initial values and

Table 6.3 Initial values and terminal constraints

Variable	Initial value $t = 0$	Terminal value $t = 70$
$K(t)$	10	≥ 15
$M(t)$	2.5	≤ 2.5
$R(t)$	1.5	≥ 0
$g(t)$	0.5	Unconstrained
$b(t)$	0.8	Unconstrained

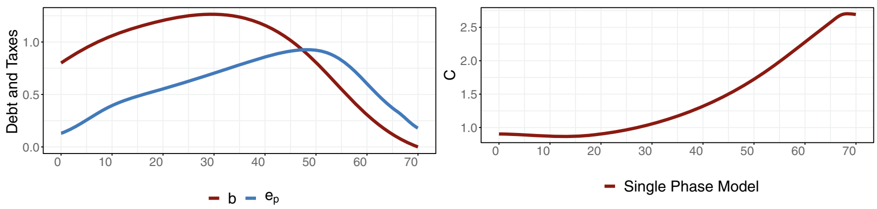

(a) Government debt, b and tax, e_P (b) Consumption, C

Fig. 6.1 Government debt, taxes and consumption in single-regime model

terminal constraints are listed in Table 6.3. Note that the terminal constraints ensure that there is at least a 50% increase in private capital over the 70-year period and that CO_2 concentration will only increase slightly over the entire period. In other words, the parameterizations presume climate action is successful. This differs from the setup in Semmler et al. [15] which considered climate policy optimization against a baseline of "business as usual" (i.e. no investment in climate change policies).

Figure 6.1 shows the trajectories of government debt b, taxes e_P and consumption C over the full horizon. Government debt at first rises as various investments are made, but as the terminal point $t = T$ approaches, public debt is driven toward zero so that there are no outstanding obligations at the end of the finite horizon (i.e. no Ponzi schemes are allowed). This downward trend to $b(T) = 0$ is driven by increase is the tax rate e_P which peaks at $t = 48$. Throughout this trajectory consumption increases as it is the major component of welfare in (6.7).

The positive consumption growth rate in the face of increasing taxation comes at the cost of lower investment in capital—both private and public. Figure 6.2 shows the trajectory of private capital stock K. After an initial, brief contraction K increases by approximately 60%. But, in the final 11 periods of the model, the tax burden takes its toll and private capital falls rapidly, and then recovers slightly toward its terminal constraint $K(T) = 15$. Public capital follows a similar pattern, albeit without the slightly recovery at the terminal point. It increases from $g(0) = 0.5$ to $g(56) = 1.2$, only to fall back slightly in the final years of model. The retrenchment is more dramatic for g than it is for K, with public capital stock reaching 0.89 at the terminal point.

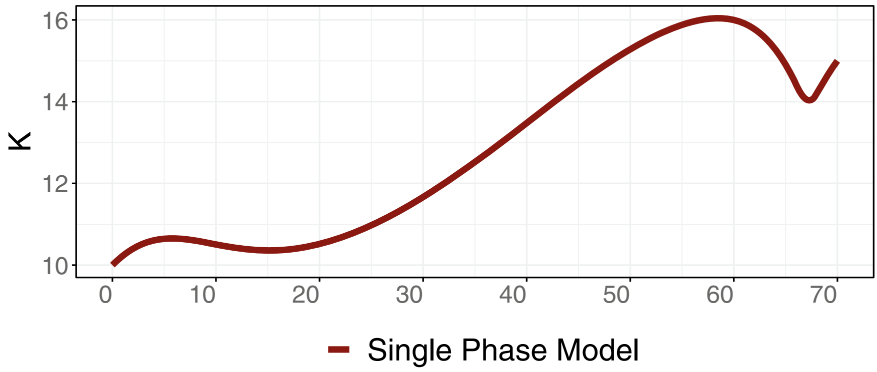

Fig. 6.2 Private capital stock in single-regime model

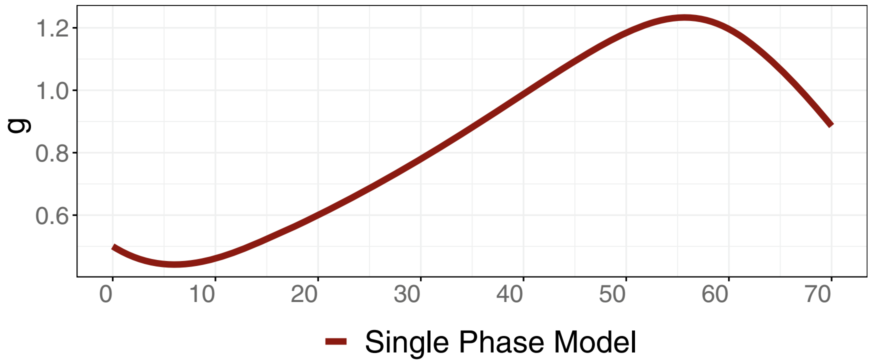

Fig. 6.3 Public capital stock in single-regime model

In addition to reducing the private and public capital stocks, the increased tax revenue needed to pay off government debt has another perverse impact: increasing CO_2 emissions. Recall that private capital K is a carbon-neutral input for the production of Y, with the extracted non-renewable resource u being the alternative input.[7] We find that $u(t) \approx 0$ for $t < 67$, but becomes positive thereafter. At $t = 67$ the extraction rate u rapidly increases (see Fig. 6.4). This behaviour in the model's final decade is driven by the shift in production toward fossil fuel inputs that allow the economy to achieve the no-Ponzi condition $b(T) = 0$ without negatively impacting consumption (Fig. 6.3).

[7]See Eq. (6.6) and accompanying text. We also want to note the long period of no fossil fuel energy extraction comes from the fact that the carbon stock is presumed to start at a low initial level as well as the low efficiency of the fossil fuel-based energy assumed, i.e. $A_u = 100$ (see Sect. 6.6 below).

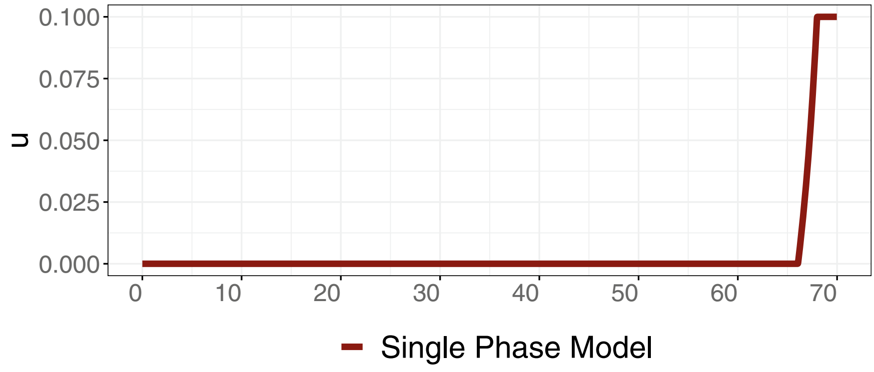

Fig. 6.4 Non-renewable resource extraction rate in single-regime model

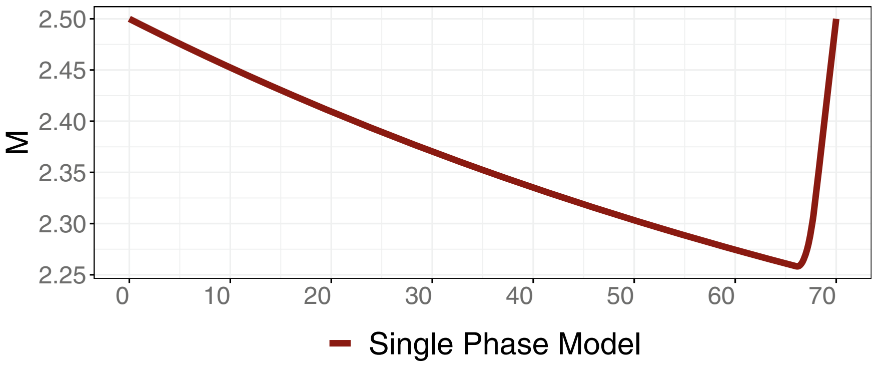

Fig. 6.5 CO_2 emissions in single-regime model

The sudden jump in u translates into additional carbon emissions M. Figure 6.5 shows that reliance on K in production corresponds with a steady decline in CO_2 emissions. This decline is completely reversed by the re-introduction of u in production. Evidently, the somewhat generous terminal condition applied to $M(T)$ allows for this fossil fuel-intensive behaviour.

Finally, Fig. 6.6 shows the relative allocation of g to infrastructure ν_1, adaptation efforts ν_2 and emissions mitigation ν_3. The results are consistent with those reported in Semmler et al. [15]. Namely, approximately 96% of g is allocated to ν_1, 4% to ν_2 and essentially 0% to ν_3 during the first 57 periods. For $t > 60$, ν_1 declines slightly as K falls to it terminal value and adaptation efforts ν_2 increase slightly as non-renewable extraction rates increase (see Fig. 6.4).

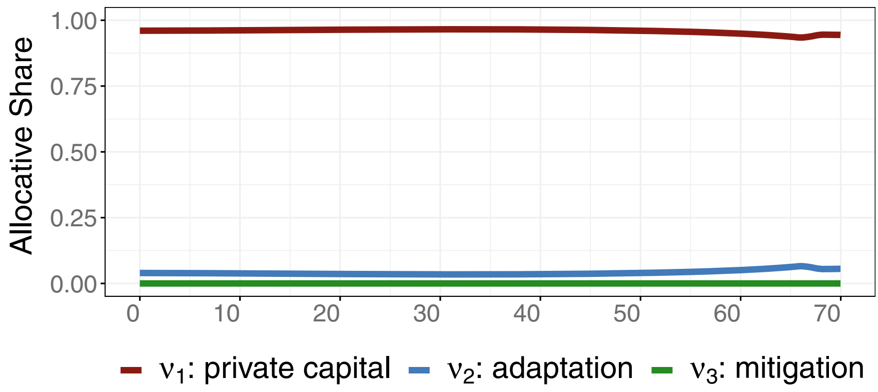

Fig. 6.6 Optimal distribution of public capital in single-regime model

6.5 Multi-phase Extension of the Model

The multi-phase model uses the same parameterization listed in Table 6.2, as well as the same initial values and terminal constraints in Table 6.3.[8] As discussed in Sect. 6.5 and Appendix, the nonlinear multi-phase problem is solved using the arc parameterization method (APM). In accordance with the continuity condition in (6.10), the state variables transition continuously between regimes. However, the model solution generates discontinuous jumps in the controls variables. This is a natural result of the changed dynamic system introduced as the model shifts from one policy environment to another.[9]

The multi-regime model presented here assumes fixed switching points. While it is computationally feasible for the transition times to be endogenously and optimally determined as part of the dynamic system's solution [12], we do not allow for this extra complexity here. Beyond the greater computational expense, preliminary testing indicates that time spent in the second regime (when green bonds are issued) is maximized. This is not surprising as this regime is not constrained by the no Ponzi condition. However, such a result is neither realistic nor helpful as the dynamics of the two other, extremely short regimes become impossible to discern. The three regimes are thus fixed on the intervals $t \in [0, 20]$, $t \in (20, 40]$ and $t \in (40, 70]$.

[8]Of course, the initial values apply only to the starting values in phase 1 and the terminal constraints bind only at $T = 70$, at the end of the third phase.

[9]DSGE models have also recently allowed for regime switches (see [8], Sect. 7.2), but not address the issue of discontinuities in the control variables.

6.5.1 Regimes of the Multi-phase Model

The first phase, "no green bonds", corresponds exactly to the single-phase model discussed in Sect. 6.4. In particular, $\varsigma_k = \tau_k = 0$ for $k = 1$. In the second phase, $k = 2$, green bonds are introduced as a financing option $\varsigma_2 > 0$. We choose the specific value $\varsigma_2 = 0.05$. The long-term nature of the green bonds means no repayments are made in $k = 2$, such that $\tau_1 = \tau_2 = 0$. In the third and final phase the green bonds come due and the government ceases issuance, $\varsigma_3 = 0$. Repayment is conducted through a special income tax set at 3%, $\tau_3 = 0.03$. Although the accumulated green bond debt feeds into the same overall public debt level, b, the special tax τ_k provides the policymaker with a new mechanism by which to raise revenue. The policymaker can of course continue to control the value of capital taxation e_P throughout the model's three phases.

The introduction of a new asset—green bonds—has implications for financial markets. In general, the issuance of the new green bonds—especially when scaled up—will have price and rebalancing effects on the asset market.[10] In our context we assume that wealth-holders have many assets in their portfolio, such as cash, equity, real estate and bonds. Further, we assume all green bonds are sold at issuance, which implies that wealth-holders bid prices down to a market clearing level. This affects the relative price and return across assets, but can simply be thought of as causing a rebalancing of different types of assets in the portfolio. A similar but more static approach is considered by Tobin [16] in macroeconomic portfolio theory where asset accumulation and portfolio allocation decisions interact with the real side of the economy. A dynamic extension of Tobin's approach is developed in Chiarella et al. [3] in which there are simultaneous asset accumulation and dynamic portfolio decisions.[11]

In the graphical results that follow, the first phase in which no green bonds have been issued is plotted in red. The second phase—green bond issuance—is coloured green, and the third phase, repayment, is blue.

6.5.2 Multi-phase Model Results

As in the single-regime model, government debt b builds up rapidly before being driven to the no-Ponzi condition $b(T) = 0$. However, the trajectory of b is somewhat

[10] In addition, when green bonds portend reductions in CO_2-emitting energy sources, their issuance might lead to significant devaluation of assets representing fossil fuels if this is expected to increase the risk of these assets becoming (so-called) "stranded" assets. Formally introducing this effect is left for later work.

[11] Note that in the present context the Ricardian equivalence theorem, which says that the real side of the economy will not be affected by deficit spending financed through issuing of bonds, is not applicable in this context. This is because green bonds are used to reduce future damages to GDP, and thus carry some future returns from their investments (in particular from public infrastructure). For details, see Orlov et al. [13].

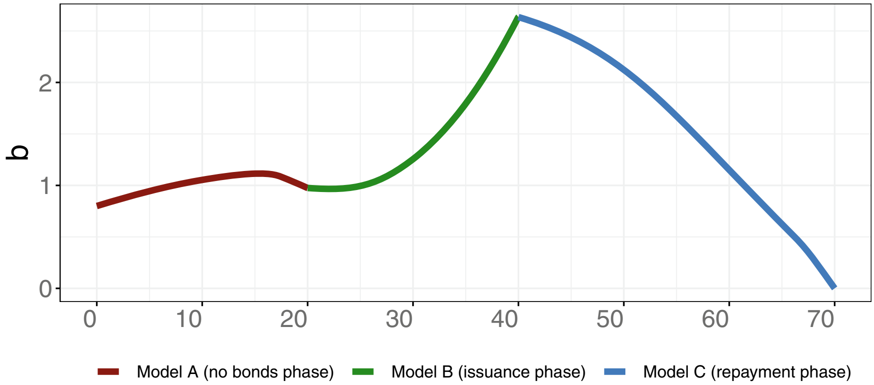

Fig. 6.7 Public debt in 3-regime model

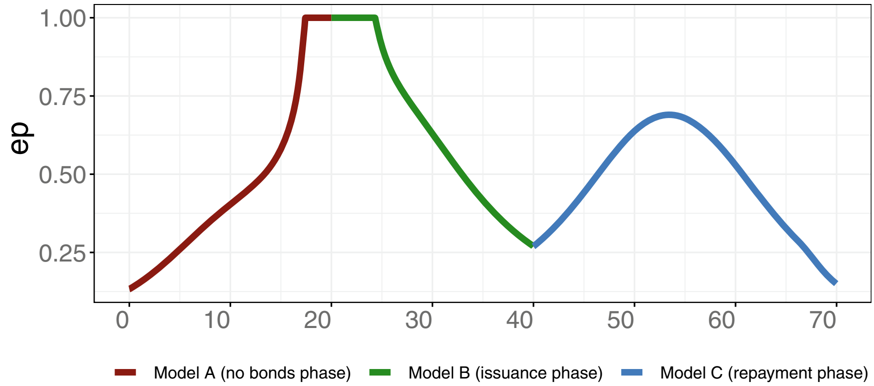

Fig. 6.8 Capital taxation level in 3-regime model

different and specific to the three regimes (see Fig. 6.7). In the first phase, government debt b increases only mildly and even decreases mildly ahead of the green bond issuance phase. Unsurprisingly, the introduction of green bonds increases the stock of public debt threefold to 2.6. The debt level reverses course only as the repayment phase is introduced at $t = 40$.

Interestingly, the standard taxation rate chosen by the policymaker follows a rather different path than before. Figure 6.8 shows e_P rising rapidly at the end of phase 1 and hits the constraint $e_P \leq 1$. The introduction of green bonds allows for the rapid reduction of taxation rates. In the final phase, standard taxation rates increase so as to help reduce the overall tax burden.

Consumption follows a similar upward trajectory in the first and second regimes, but then retrenches slightly in the third phase (see Fig. 6.9). The fall in per capita consumption in $k = 3$ is due to the reduction in output Y stemming from the special tax τ_k. Yet, at its peak per capita consumption reaches $C = 2.97$, surpassing the maximal

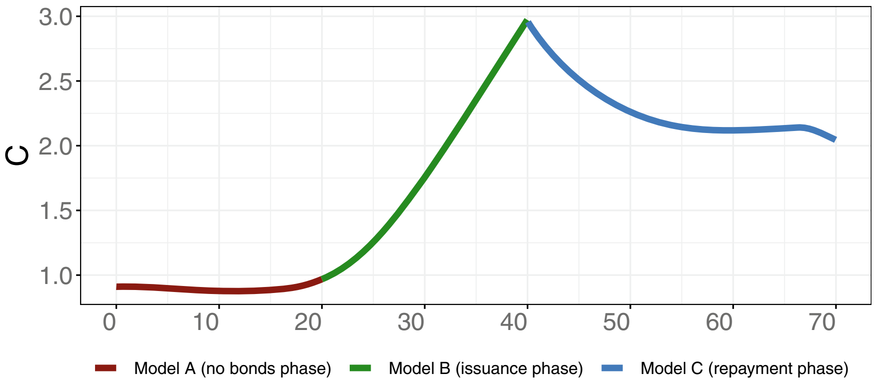

Fig. 6.9 Consumption in 3-regime model

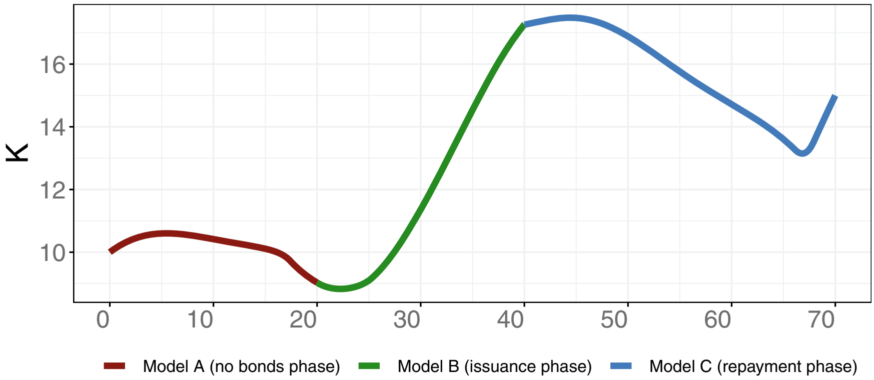

Fig. 6.10 Private capital stock in 3-regime model

observed in the single-phase model, $C = 2.70$. This higher maximal consumption contributes to the overall welfare improvement of the multi-phase model relative to the single-phase version (see Sect. 6.5.3).

Both private and public capital follow as similar pattern as seen in the single-regime model: a rapid increase over the first two-thirds of the finite horizon is reversed with a retrenchment in both as $t \to T$. As before, the retrenchment of private capital K is partially reversed in the final stages of the model (Fig. 6.10), whereas public capital declines monotonically during the third phase (Fig. 6.11).

Carbon dioxide emissions M follow a nearly identical pattern trajectory in the three-regime model in Fig. 6.12 as in the single-regime model (see Fig. 6.5). As before, the terminal value $M(T) = 2.5$ is the reason for the sudden jump in emissions. This constraint can be thought of as a politically determined contract to limit emissions at a higher than optimal level. Where a lower political bound for emissions agreed upon, the final level of emissions modelled would of course be lower as well.

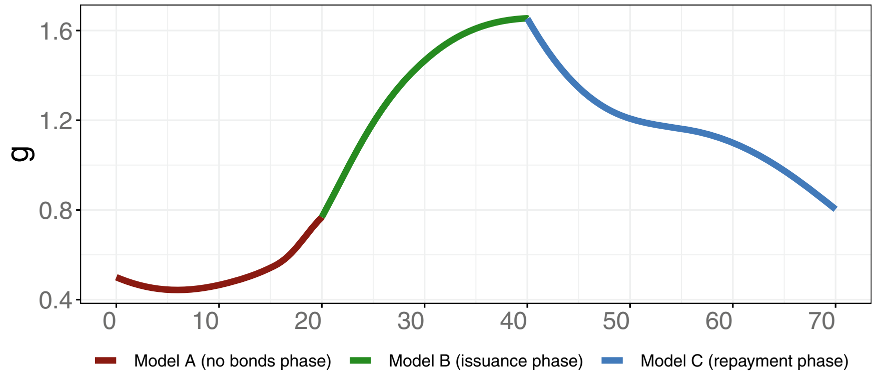

Fig. 6.11 Public capital stock in 3-regime model

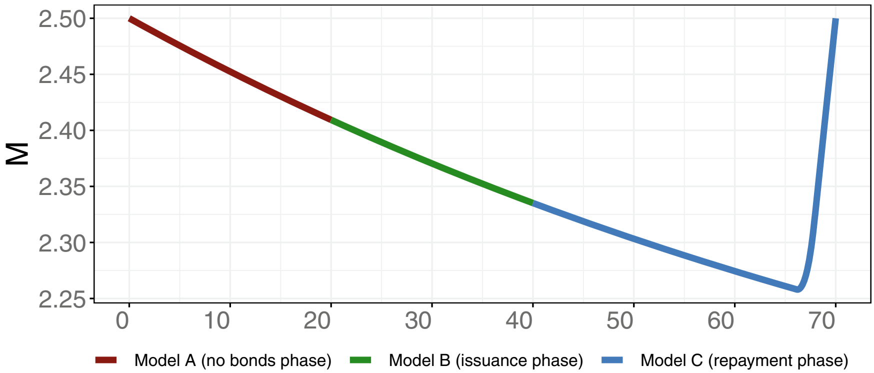

Fig. 6.12 Carbon dioxide emissions in 3-regime model

Figure 6.13 displays some of the discontinuities of the ν_i control variables as the system enters a new regime. In particular, the third regime exhibits additional investments in adaptation efforts, which then slowly reduces as $t \to T$. Mitigation efforts remain steady and around zero throughout the three regimes. The effect of these shifts in allocations is to reduce the rate of investment of public capital g into green infrastructure K relative to the single-phase model (see Fig. 6.6). The average allocation to K is slightly lower at approximately 94% in the multi-regime model versus 95% in the single-regime model.

6.5.3 Comparison of Welfare Results

The single and multi-regime models share similar overall pathways, but the slight differences accumulate to large total welfare differentials (see Table 6.4). Average

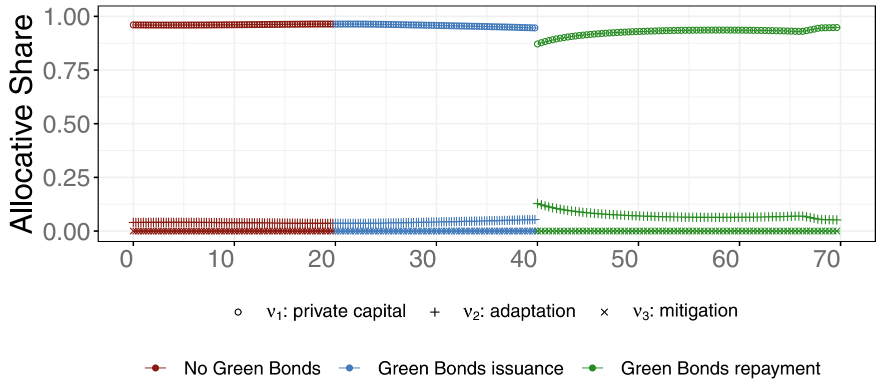

Fig. 6.13 Optimal allocation of public capital

Table 6.4 Single and multi-phase model key variable comparison

		Average	Terminal	Maximum
Single regime				
Consumption	C	1.42	2.69	2.70
Private capital	K	12.82	15.00	16.04
Public capital	g	0.85	0.89	1.23
Carbon emissions	M	2.36	2.50	2.50
Multi-regime				
Consumption	C	1.66	2.05	2.97
Private capital	K	12.63	15.00	17.48
Public capital	g	1.02	0.80	1.65
Carbon emissions	M	2.38	2.50	2.50
Social welfare		*Total*		
Single regime	W	−21.48		
Multi-regime	W	−12.34		

consumption over time was higher in the multi-regime model (1.7 versus 1.4), as is the single-period maximum value (3.0 vs. 2.7). The stock of private and public capital shifted from the single to the multi-regime model. Average K declined slightly in the multi-regime model, whereas average g increased when green bonds were introduced. As expected, from the trajectories observed above, CO_2 concentration levels are virtually identical in the two models, which the multi-regime model exhibiting marginally higher average M (2.38 vs. 2.36).

The higher average pathway of C generated a significantly higher overall social welfare value for the multi-regime model. The values calculated from Eq. (6.7), show that the multi-regime model is superior with at $W_{multi}(T; X; U) = -12.3$ as compared to the single-regime model's total welfare value of $W_{single}(T; X; U) = -21.5$.

6.6 Sensitivity Analysis

Finally, we present here some sensitivity analyses of the multi-phase IAM. The focus is on the efficiency index of A_u, which sets the relative productivity level of the non-renewable resource in production. The model results discussed above set $A_u = 100$. We compare the trajectories for several key variables with higher non-renewable input productivity, for $A_u = 300$ and $A_u = 500$. This is a particularly important parameter to test since there was little extraction and use of the non-renewable resource under the initial parameterization. Unsurprisingly, for higher A_u parameterizations the extraction rate u becomes substantially higher.

With a more productive non-renewable resource, production uses a greater level of u as an input (see Eq. 6.6). The direct result of this is the increased level of CO_2 emissions in the atmosphere. Figure 6.14 shows emissions falling persistently in the baseline case $A_u = 100$ (in red) until the terminal constraint pulls it up in the final periods. For $A_u = 300$ (in green) and $A_u = 500$ (in blue), emissions rise rapidly in the early phases of the model before trending down to the fixed terminal point $M(T) = 2.5$.

The six panels in Fig. 6.15 show the pathways under $A_u = 100$, 300 and 500 for public g and private K capital, consumption C and public debt b, and the allocation of public capital productivity enhancements ν_1 and climate change mitigation ν_3. In general, the large change (a 3- to 5-fold increase) in the A_u efficiency index leads to relatively small shifts in these variables' pathways. Further, in each case the shift in trajectories move the expected direction. Public and private capital accumulation rises faster and peaks at a higher level as one of the inputs to production is made cheaper (viz. more productive). Consumption is higher in all periods as A_u rises, and the allocation to productivity-enhancing capital ν_1 falls relative to the baseline as the higher carbon emissions rise. In place of ν_1, public capital is shifted toward greater CO_2 mitigation efforts, ν_3, in the third phase of the model as a response to the higher emissions generated from non-renewable resource-intensive production.

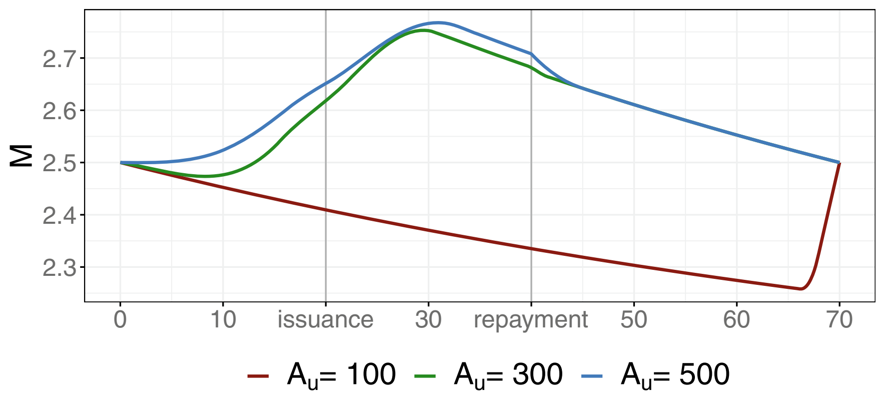

Fig. 6.14 Sensitivity test of CO_2 emissions

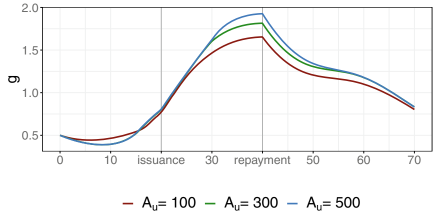

(a) Public Capital g

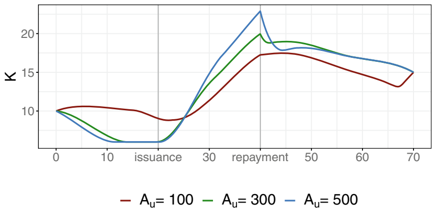

(b) Private Capital K

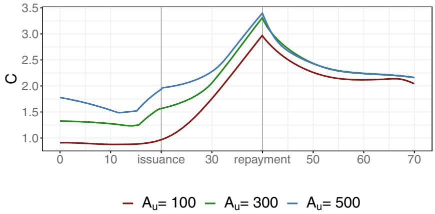

(c) Consumption C

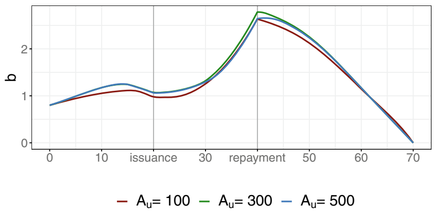

(d) Public debt, b

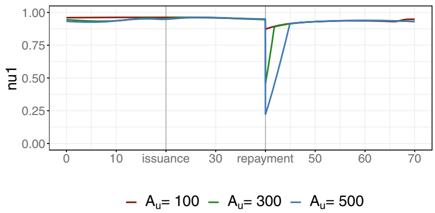

(e) Allocation to private capital ν_1

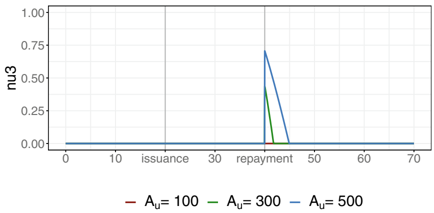

(f) Allocation to CO_2 mitigation ν_3

Fig. 6.15 Sensitivity test of selected state and control variables

6.7 Conclusion

In Semmler et al. [15] we developed an integrated assessment model (IAM) explicitly accounting for the extraction and use in production of CO_2-emitting resources, as well as the optimal allocation of public finances to counter climate change. We have extended that IAM framework here to consider how new policies, specifically green bond financing, could be introduced to the set of available policies. To achieve this, we posited a 3-regime model in which green bonds are (i) non-existent, (ii) issued and (iii) repaid. The multi-regime model was shown to be Pareto-superior to the single-regime baseline, and enhanced intergenerational equity.[12]

Overall, the IAM developed here is an advancement both in terms of the solution algorithm employed and in its use of novel, multi-phase dynamics (namely, APM). As mentioned, the modelling of non-renewable resource extraction and detailed public

[12] In this context, a recent discussion of proposals for central banks to accept climate bonds as collateralizable securities is available in Flaherty et al. [6].

sector policies on climate change are new but important features in the IAM literature. In addition we have treated the damage function of climate change as impacting social welfare directly, as opposed to indirectly through reductions in the rate at which output is produced. While neither approach is perfect, we have employed the direct-utility impact version because we believe it is better able to capture the multitude of physical, ecological and societal losses that are likely to be induced by unabated climate change. Regardless of how the damage function is introduced, our framework allows for a multi-phase approach in which new, unforeseen policies, events and dynamics of the state equations can be introduced and responded to by the policymaker oriented toward a limited time horizon. We believe this to be a far more natural framework to address climate-economic-financial questions over a known, finite period of time.

Appendix: Multi-phase Optimal Control Problems and Their Numerical Solution

Multi-process (multi-phase) optimal control problems have been studied by Clarke and Vinter [4, 5] and later by Augustin and Maurer [1]. Suppose that a dynamic economic process on a given time interval $[0, T]$ consists of $(s+1)$ phases (regimes) that switch at the transition times $t_k \in (0, T),\ k = 1, ..., s$. The switching times are ordered according to

$$0 = t_0 < t_1 < t_2 < \cdots < t_s < t_{s+1} = T. \tag{6.11}$$

In each interval $[t_k, t_{k+1}],\ k = 0, 1, \ldots s$, the dynamics and objectives may be different.

Let $x \in \mathbb{R}^n$ be the state variable and $u \in \mathbb{R}^m$ the control variable. The dimensions of the state vector and control vector may be different in different phases. For simplicity, we refrain here from discussing this general case and assume the same dimensions in each subinterval. Hence, the dynamics of the economic process in the interval $[t_k, t_{t+1}]$ is given by the ordinary differential equation,

$$\dot{x}(t) = f_k\big(x(t), u(t)\big), \quad t_k \le t \le t_{k+1} \quad (k = 0, 1, \ldots, s), \tag{6.12}$$

where the right-hand side of the ODE is a C^1 function $f_k : \mathbb{R}^n \times \mathbb{R}^m \to \mathbb{R}^n$. The time t_k in (6.12) is understood from the right, while the time t_{k+1} is taken from the left. The initial condition and terminal constraints are given as

$$x(0) = x_0, \quad \psi(x(T)) = 0. \tag{6.13}$$

We further impose control constraints in each interval,

$$u_{k,\min} \le u(t) \le u_{k,\max}\,, \quad t_k \le t \le t_{k+1} \quad (k = 0, 1, \ldots, s), \tag{6.14}$$

with $-\infty \le u_{k,\min} < u_{k,\max} \le +\infty$.

A *continuous* state trajectory $x(t)$ on the whole interval $[0, T]$ is obtained by imposing the continuity condition

$$x(t_k) = x(t_k-), \qquad k = 1, \ldots, s. \tag{6.15}$$

Note that the continuity of the state variables in (6.15) does not automatically ensure the continuity of the control variables; in fact, these can jump, as we demonstrate below, when the system transitions between policy phases are studied. Moreover, we can prescribe interior (transition) conditions for the state variables by

$$\varphi_k(x(t_k-) = 0, \quad k = 1, \ldots, s, \tag{6.16}$$

with C^1 functions $\varphi_k : \mathbb{R}^n \to \mathbb{R}$.

In each interval one may also have different objectives which are defined by functions $L_k : \mathbb{R}^n \times \mathbb{R}^m \to \mathbb{R}^n$, $k = 0, 1, \ldots, s$. Then the optimal multi-phase control problem is defined by the following objective:

$$J(x, u) = \max_u \left\{ \sum_{k=0}^{k=s} \int_{t_k}^{t_{k+1}} e^{-r_k \cdot t} L_k(x(t), u(t))\, dt \right\}, \tag{6.17}$$

subject to the constraints (6.12)–(6.15), and $r_k > 0$ for $k = 0, 1, \ldots, s$.

To solve the optimal multi-phase control problem, we implement the arc-parametrization in Maurer et al. [12] in conjunction with discretization and nonlinear programming methods. Although they apply the arc-parametrization method (APM) only to bang-bang control problems, the APM can easily be extended to continuous, multi-phase control problems as follows. Let

$$\xi_k = t_{k+1} - t_k, \quad k = 0, 1, \ldots, s, \tag{6.18}$$

denote the *arc lengths* (or, arc durations) of the multi-process. The time interval $[t_k, t_{k+1}]$ is mapped onto the fixed interval $[k/(s+1), (k+1)/(s+1)]$ by the linear transformation

$$t = a_k + b_k \tau, \quad \tau \in \left[\frac{k}{s+1}, \frac{k+1}{s+1} \right], \tag{6.19}$$

where $a_k = t_k - k\xi_k$ and $b_k = (s+1)\xi_k$. Taken together, the complete time interval $[0, T]$ is thereby mapped onto the unit interval $[0, 1]$. Identifying $x(\tau) = x(a_k + b_k\tau) = x(t)$ in the relevant intervals, we obtain the scaled ODE system

$$\frac{dx}{d\tau} = \xi_k(s+1) \cdot f_k\big(t_k + \tau \cdot \xi_k, x(\tau), u(\tau)\big) \tag{6.20}$$

for $\tau \in \left[\frac{k}{s+1}, \frac{k+1}{s+1}\right]$. Note that ξ_k are treated as optimization variables if the transition times t_k are free.

The time transformation leads us to rescale the objective function (6.17) as follows:

$$J(x,u) = \max_u \left\{ \sum_{k=0}^{k=s} \int_{\frac{k}{s+1}}^{\frac{k+1}{s+1}} \xi_k(s+1) e^{-r_k \cdot (a_k + b_k \tau)} L_k(x(\tau), u(\tau))\, d\tau \right\}, \tag{6.21}$$

and subject to (6.12)–(6.15) and rescaled according to (6.19). For the purposes of exposition, we fix the transition points t_k to reflect the exogenous (and often sub-optimally protracted) nature of introducing and implementing new policies.

References

1. Augustin, D., & Maurer, H. (2000). Second order sufficient conditions and sensitivity analysis for optimal multiprocess control problems. *Control and Cybernetics*, *29*, 11–31.
2. Bonen, A., Semmler, W., & Klasen, S. (2014). *Economic damages from climate change: A review of modeling approaches*. SCEPA working paper 2014–03, Schwartz Center for Economic Policy Analysis.
3. Chiarella, C., Semmler, W., Hsiao, C.-Y., & Mateane, L. (2016). *Sustainable asset accumulation and dynamic portfolio decisions*. Springer.
4. Clarke, F. H., & Vinter, R. B. (1989). Applications of optimal multiprocesses. *SIAM Journal of Control and Optimization, 27*, 1048–1071.
5. Clarke, F. H., & Vinter, R. B. (1989). Optimal multiprocesses. *SIAM Journal of Control and Optimization, 27*, 1072–1091.
6. Flaherty, M., Gevorkyan, A., Radpour, S., & Semmler, W. (2017). Financing climate policies through climate bonds: A three stage model and empirics. *Research in International Business and Finance*, *42*, 468–479.
7. Heine, D., Semmler, W., Mazzucato, M., Braga, J. P., Flaherty, M., Gevorkyan, A., et al. (2019). Financing low-carbon transitions through carbon pricing and green bonds. *Quarterly Journal of Economic Research*, *88*, 29–49.
8. Herbst, E., & Schorfheide, F. (2015). *Bayesian estimation of DSGE models*. Princeton University Press.
9. Hotelling, H. (1931). The economics of exhaustible resources. *Journal of Political Economy*, *39*(2), 137–175.
10. Lin, Q., Loxton, R., & Teo, K. L. (2014). The control parameterization method of optimal control problems: A survey. *Journal of Industrial and Management Optimization*, *10*, 275–309.
11. Loxton, R., Lin, Q., Rehbock, V., & Teo, K. L. (2012). Control parameterization for optimal control problems with continuous inequality constraints: New convergence results. *Numerical Algebra, Control and Optimization*, *2*, 571–599.
12. Maurer, H., Büskens, C., Kim, J.-H., & Kaya, C. Y. (2005). Optimization methods for the verification of second order sufficient conditions for bang-bang controls. *Optimal Control: Applications and Methods*, *26*, 129–156.

13. Orlov, S., Rovenskaya, E., Puascunder, J., & Semmler, W. (2018). *Green bonds, transition to a low-carbon economy, and intergenerational fairness: Evidence from an extended dice model*. IIASA working paper.
14. Sachs, J. (2014). Climate change and intergenerational well-being. In L. Bernard & W. Semmler (Eds.), *The Oxford handbook of the macroeconomics of global warming* (pp. 248–259). Oxford University Press.
15. Semmler, W., Maurer, H., & Bonen, A. (2018). An extended integrated assessment model for mitigation & adaptation policies on climate change. In G. Feichtinger, R. Kovacevic, & G. Tragler (Eds.), *Control systems and mathematical methods in economics* (Vol. 687). Lecture notes in economics and mathematical. Springer.
16. Tobin, J. (1969). A general equilibrium approach to monetary theory. *Journal of Money, Credit and Baking*, *1*(1), 15–29.